Thermo-responsive lipophilic NIPAM-based block copolymers as stabilizers for lipid-based cubic nanoparticles

Arianna Balestri, Barbara Lonetti, Simon Harrisson, Barbara Farias-Mancilla, Junliang Zhang, Heinz Amenitsch, Ulrich Schubert, Carlos Guerrero-Sanchez, Costanza Montis, Debora Berti

Thermo-responsive lipophilic NIPAM-based block copolymers as stabilizers for lipid-based cubic nanoparticles

Arianna Balestri[a], Barbara Lonetti[b]*, Simon Harrisson[c], Barbara Farias-Mancilla[b], Junliang Zhang[d], Heinz Amenitsch[e], Ulrich Schubert[f], Carlos Guerrero-Sanchez[f], Costanza Montis[a]*, Debora Berti[a]

[a] Department of Chemistry "Ugo Schiff", University of Florence and CSGI, Florence, Italy; [b] IMRCP, UMR5623 CNRS, Université de Toulouse, Toulouse, France; [c] LCPO, UMR 5629 CNRS, ENSCBP, University of Bordeaux, Pessac, France; [d] Shaanxi Key Laboratory of Macromolecular Science and Technology, Northwestern Polytechnical University, Xi'an, Shaanxi, China; [e] Institute of Inorganic Chemistry, Graz University of Technology, 8010 Graz, Austria;[f] IOMC and JCSM, Friedrich Schiller University of Jena, Jena, Germany;

Total number of words: 6555

Total number of tables/figures: 8

Abstract

The design of drug delivery systems (DDS) for the encapsulation of therapeutic and the controlled release to the target site of the disease is one of the main goals in nanomedicine. Although already explored in an extensive number of studies over the years, lipid assemblies, and particularly liposomes, are still considered the most promising and interesting candidates as DDS due to their biocompatibility and structural similarity with plasma membranes. Lately, this research area has been extended to include more complex lipid assemblies, such as cubosomes. Cubosomes are considered to date an emerging structural platform for the delivery of molecules with pharmaceutical interest, such as drugs, bioactive and contrast agents. Here we report on the application of a recently synthesized thermo-responsive copolymer poly(N,N-dimethylacrylamide)-*block*-poly(N-isopropylacrylamide) (PDMA-*b*-PNIPAM), as a thermoresponsive stabilizer of lipid-based nanoparticles for drug-delivery. First, we assessed the affinity of PDMA-*b*-PNIPAM towards supported and free-standing bilayers; then, we explored the colloidal and thermoresponsive properties of cubic self-assembled DDS composed of glycerol-monooleate (GMO), where PDMA-*b*-PNIPAM replaces the conventional stabilizer Pluronic F127 (PEOx-PPOy-PEOx), normally used for cubosomes. We prepared dispersions of cubic lipid nanoparticles with two kinds of PDMA-*b*-PNIPAM block copolymers, differing by the molecular weights. The colloidal properties were then assessed and compared to those exhibited by standard lipid cubic dispersions stabilized by Pluronic

F-127, combining a series of experimental techniques (Quartz Microbalance with Dissipation monitoring, Dynamic Light Scattering, Small-Angle X-rays Scattering, Cryo-Transmission Electron Microscopy). Interestingly, PDMA-*b*-PNIPAM- stabilized cubosomes display additional benefits with respect to those stabilized by Pluronic, thanks to the combination of a "sponge "effect for the controlled release of encapsulated molecules and an increased affinity towards lipid bilayer membranes, which is a promising feature to maximize fusion with the target-cellular site.

Keywords

Cubosomes, Amphiphilic block copolymer, Stabilizer, Model membrane, Drug delivery

1. Introduction

In the last few decades, much effort has been devoted to the development of drug-delivery systems (DDSs) with the ability to encapsulate therapeutic agents of different chemical nature and to deliver them in a temporally and spatially controlled manner to their biological target [1–3]. Despite this intense research, lipid-based DDS, among the first to be developed and brought to the market, remain probably unsurpassed. In fact, thanks to biocompatibility and synthetic versatility, most FDA-approved nanomedicine formulations contain lipid assemblies [4,5]. For instance, several anticancer drugs with high toxicity and low bioavailability were delivered using a liposomal platform, overcoming their solubility and stability drawbacks [6,7]. In addition, recent FDA- and EMA-approved mRNA lipid vector-based vaccines against COVID-19 have brought renewed interest in lipid-based delivery of oligonucleotides/nucleic acids for therapeutic applications, as vaccines, antitumoral drugs and so on [8,9].

Within the field of lipid-based nanostructures, lipid vesicles, or liposomes, are the simplest and most common lipid-based systems investigated for drug delivery applications. As amphiphilic molecules, lipids in water self-assemble in a larger variety of more complex structures, such as cubic liquid crystalline mesophases, where a highly curved lipid bilayer arranges in a complex 3D structure where lipid regions and aqueous channels coexist. These complex lipid mesophases, once dispersed as nanosized particles (suitable for diverse administration routes), offer multiple advantages as DDS when compared to liposomes [10–16]. Cubic nanostructures are characterized by high internal organization, stability, versatility and tunable morphological characteristics [17]. In addition, the high membrane surface area to volume ratio of lipid cubic mesophases (400 m^2/g [18]), could dramatically improve the loading capability of both hydrophilic and hydrophobic molecules [19]. Finally, recent studies have highlighted the fusogenicity of cubic nanoparticles, potentially facilitating their cellular

uptake [20]. Given these fascinating characteristics, lipid mesophases are an emerging platform for the in-vivo delivery of pharmaceutical and imaging agents [21–25].

The unsaturated monoglyceride, glyceryl-monooleate (GMO), which is a fully biocompatible FDA-approved building block, exhibits, under excess of water, a *Pn3m* cubic liquid crystalline phase, consisting of a 3D network separating two continuous non-intersecting hydrophilic channels [26]. Cubic nanoparticles in the size range of 100-400 nm, also known as cubosomes, are typically prepared via a top-down approach [20,27], in which cubic nanoparticles are obtained by mechanical fragmentation of the lipid-water phase and successive steric stabilization. Dispersions of these cubic phases are commonly obtained with the aid of an appropriate stabilizer [28], which provides a steric and/or electrostatic-repulsive barrier between the particles without disrupting their inner structure. Steric stabilizers are most commonly employed since charged surfactant molecules often result in loss of the internal phase structure [29].

The stabilizer plays a crucial role in the behaviour of the cubic dispersion as it modulates the interactions between nanoparticles and the release of their cargo. Its function also spreads to the cellular membranes of the target-site as it controls the biocompatibility of the cubosomes in cellular environments [30]. Given the importance of steric stabilizers to the overall behaviour of cubosomes, many different compounds have been proposed to stabilize cubosomes. To date, however, only a few classes of steric stabilizers are commonly used [28]. The tri-block copolymer Pluronic F127, (PEO_{100}-*b*-PPO_{65}-*b*-PEO_{100}), is the most-applied amphiphile in the stabilization of cubosomes. Its PPO block is located at the surface of the dispersed cubic phase or within the bilayer, while its PEO portions protrude towards the bulk aqueous phase [31]. Alternative stabilizers have been proposed to allow controlled release of guest molecules in response to external stimuli and to improve their interaction with bio-interfaces. For example, new biocompatible formulations were formed by dispersing the lipids glyceryl monooleate (GMO) and phytantriol (PHYT) with biodegradable stabilizers, reducing their cytotoxicity towards cells [32,33]. The inclusion of a thermo- or pH-responsive part into the steric corona of the stabilizer has also been proposed in order to obtain a stimuli-responsive behaviour [25]–[27].

In this contribution, we test a thermo-responsive block copolymer, poly(N,N-dimethylacrylamide)-block-poly(N-isopropylacrylamide) (PDMA-*b*-PNIPAM) as a novel steric stabilizer for cubosomes. This copolymer contains a thermo-responsive segment (i.e. PNIPAM), which changes its polarity from hydrophilic to hydrophobic when temperature increases from room temperature to physiological temperature [37]. The hydrophilic part of PDMA-*b*-PNIPAM presents amide pendant groups, which might improve its ability to interact with target lipid membranes compared to Pluronic-127, whose hydrophilic part is composed of PEO [38,39]. Using a combination

of complementary experimental techniques (Dynamic Light Scattering (DLS), Quartz Crystal Microbalance with Dissipation monitoring (QCM-D), Small-Angle X-ray Scattering (SAXS), Cryogenic Transmission Electron Microscopy (Cryo-EM)), we investigate: (i) the interaction of the copolymer with a lipid interface; (ii) its ability to stabilize cubosomes; (iii) the thermoresponsivity of cubosomes; and (iv) the ability of cubosomes to interact with a biomimetic lipid membrane. Our results show that PDMA-*b*-PNIPAM is a promising stabilizer for cubosomes, endowing them with a remarkable thermoresponsivity and enhancing their affinity towards biological membranes.

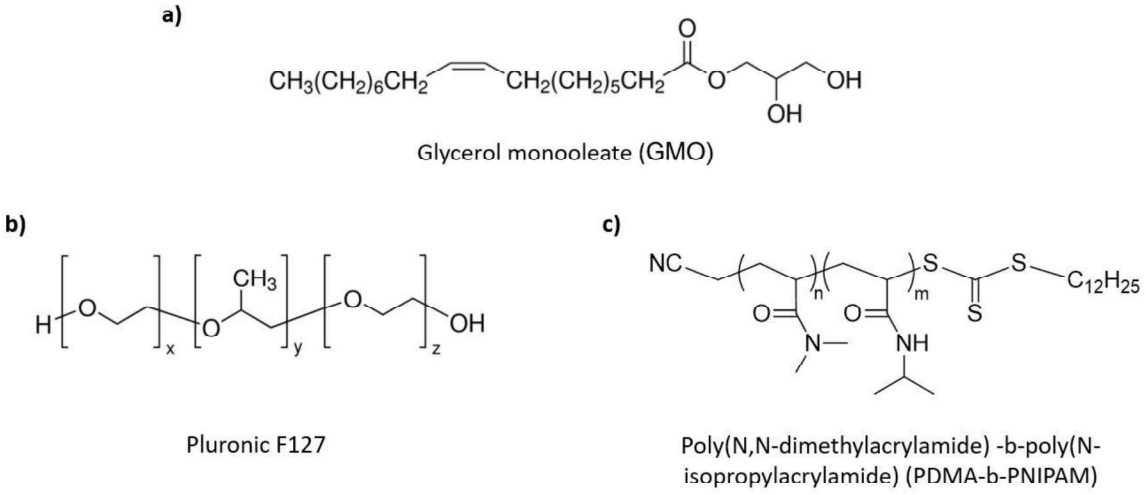

Figure 1. *Chemical structures of the lipid glycerol monooleate (GMO) (a) and of the stabilizers Pluronic F127 (b) and poly(N,N-dimethylacrylamide)-block-poly(N-isopropylacrylamide) (PDMA-b-PNIPAM)(m =50 and n =44 for B10K and, m = 110 and n = 85 for B20K) (c).*

2. Materials and methods

2.1 Materials

Glycerol monooleate (GMO) and Pluronic F127 were purchased from Croda and BASF, respectively. The block copolymer poly(N,N-dimethylacrylamide)-block-poly(N-isopropylacrylamide) (PDMA-b-PNIPAM) is a non-commercial copolymer synthesized via RAFT polymerization mediated by cyanomethyl dodecyl trithiocarbonate at 80°C (see SI for more details about the synthetic procedure). Two block copolymers were used with number average molar mass of 10 and 20 kg mol^{-1} (B10K and B20K, respectively). The phospholipid 1,2-dioleoyl-sn-glycero-3-phosphocholine (DOPC) employed for the formation of a supported lipid bilayer (SLB) was purchased from Avanti Polar Lipids (Alabama).

2.2 Lyotropic liquid crystalline nanoparticles

Lyotropic liquid crystalline nanoparticles were prepared using a top-down approach [40] starting from the preparation of the bulk crystalline phase and then its dispersion in aqueous solution up to a lipid concentration of 60 mg/ml . Three polymer/lipid compositions were prepared (20/80; 33/66 and 50/50 w/w%) with polymers PDMA-*b*-PNIPAM B10K and B20K and the lipid GMO; these systems were compared to the common Pluronic F127/GMO formulation (20/80 w/w%) (further details about compositions are reported in Table S1).

2.3 Small-Angle x-ray Scattering (SAXS)

Lipid dispersions were studied at the SAXS beamline of synchrotron radiation Elettra, Trieste (Italy) operated at 2 GeV and 300 mA ring current. Samples were introduced in a 1.5 mm glass capillary and SAXS curves were recorded at a λ = 1.5 Å using a Pilatus 3 1M detector in q-range from 0.009 $Å^{-1}$ to 0.7 $Å^{-1}$. The thermal behaviour of colloidal dispersions was evaluated using a thermostat from 25 °C to 60 °C with temperature increment of 5 °C and an equilibration time of 5 minutes for each temperature step.

2.4 Dynamic Light Scattering (DLS)

DLS was used to evaluate the z-averaged size and polydispersity of the colloidal dispersions, was performed using a Brookhaven Instrument (BI 900AT correlator and BI 200 SM goniometer). The light source was the second harmonic of a diode Nd:YAG laser, λ = 532 nm, Coherent DPY315M-100, linearly polarized in the vertical direction. The normalized intensity time autocorrelation of the scattered light was measured at 90° and analysed according to the Siegert relationship, which connects the first order or field-normalized autocorrelation function $g_1(q, \tau)$ to the measured normalized autocorrelation function $g_2(q, \tau)$:

$$g_2(q,\tau) = 1 + \beta |g_1(q,\tau)|^2 \quad (1)$$

with β being the spatial coherence factor, which depends on the geometry of the detection system. The field autocorrelation functions were analysed through a cumulant analysis stopped at the second order and through reverse Laplace transform performed with the Contin algorithm [41]. Measurements were performed on dilutes samples (1:60) to rule out multiple scattering.

2.5 Cryo-Transmission Electron Microscopy (Cryo-TEM)

Cryo-TEM images were collected at Florence Center for Electron Nanoscopy (FloCEN), University of Florence, on a Glacios microscope (Thermo Fisher Scientific) at 200 kV equipped with a Falcon III detector operated in counting mode. Images were acquired using the EPU software with a physical

pixel size of 2.5 Å and a total electron dose of ~50e^{-}Å^{-2} per micrograph. A volume of 3 µL of diluted cubosomes dispersion (1:6) was applied to glow-discharged Quantifoil Cu 300 R2/2 grids and plunge frozen into liquid ethane using an FEI Vitrobot Mark IV (Thermo Fisher Scientific). Excess liquid was removed by blotting for 1 s (blot force 1) using filter paper under 100% humidity and 10°C.

2.6 Quartz crystal microbalance with dissipation monitoring (QCM-D)

Quartz Crystal Microbalance with Dissipation monitoring (QCM-D) was performed with a Q-Sense Explorer instrument (Q-Sense, Gothenburg, Sweden), equipped with a flow liquid cell (0.5 mL internal volume), containing a coated quartz sensor, with a 5 MHz fundamental resonance frequency, mounted horizontally. The active surface of the sensors (≈ 1 cm^2) is coated with a thin SiO_2 layer (≈ 100 nm thick). The fundamental resonance frequencies (f) and corresponding energy dissipation factors (D) were measured for the odd overtones (3rd-11th). The sensor was placed in the chamber and Milli-Q water was injected at a low flowrate (0.1 $mLmin^{-1}$) and a stable baseline for both f and D for the harmonics was ensured before injection of the vesicles. After the complete sensor coverage with the lipid bilayer, the polymer or the cubosomes' dispersion was injected. The complete procedure for sensors cleaning and experiments was described elsewhere [42].

3. Results and Discussion

3.1 PDMA-*b*-NIPAM interaction with lipid bilayers

Figure 1c shows a representation of the chemical structure of the PDMA-*b*-PNIPAM block copolymer. This copolymer is characterized by the presence of a hydrophobic *n*-dodecyl ($C_{12}H_{25}$) moiety as end group, which might increase affinity towards a lipid membrane. The dodecyl group is connected to the thermoresponsive PNIPAM segment, which is then conjugated to a hydrophilic segment of PDMA. Here we investigated two different PDMA-*b*-PNIPAM block copolymers of different molar mass: B10K (M_w = 10 000 g mol^{-1}) and B20K (M_w = 20 000 g mol^{-1}); consisting of 50 or 110 NIPAM monomer and 44 or 85 DMA monomers for the polymer B10K and B20K, respectively.

We first tested the affinity of the two block copolymers toward a lipid bilayer composed of 1,2-dioleoyl-sn-glycerol-3-phosphocholine (DOPC), self-assembled both as supported lipid bilayers (SLBs) on a hydrophilic silicon substrate [43,44], and as free-standing bilayers in aqueous dispersions (i.e., DOPC liposomes).

The interaction of the copolymers with DOPC SLBs was investigated through QCM-D by monitoring the variation in frequency (Δf) and dissipation (ΔD) shifts of the quartz crystal sensor (see

Figure 2). The SLB was formed on the sensor according to a well-established protocol [45]. Once the bilayer had been formed (Δf = - 23 Hz), the polymer was injected at a concentration of 5 $mgml^{-1}$. Incubation of both copolymers with the SLB resulted in an increase in both the absolute value of frequency shifts (Δf) and dissipation (ΔD), suggesting significant adsorption onto the lipid membrane. After washing with water, a decrease (in absolute value) of both frequency shift and dissipation factor was observed, suggesting that rinsing results in the removal of some weakly adsorbed copolymer. However, both for B10K and B20K, a residual copolymer layer was permanently attached to the SLB, as shown by a frequency shift of -30 Hz for B10K and of -40 Hz for B20K, and by low dissipation factors, which indicates that the residual layer is firmly bound to the underlying SLB and suggests a significant affinity of the polymer towards the lipid membrane.

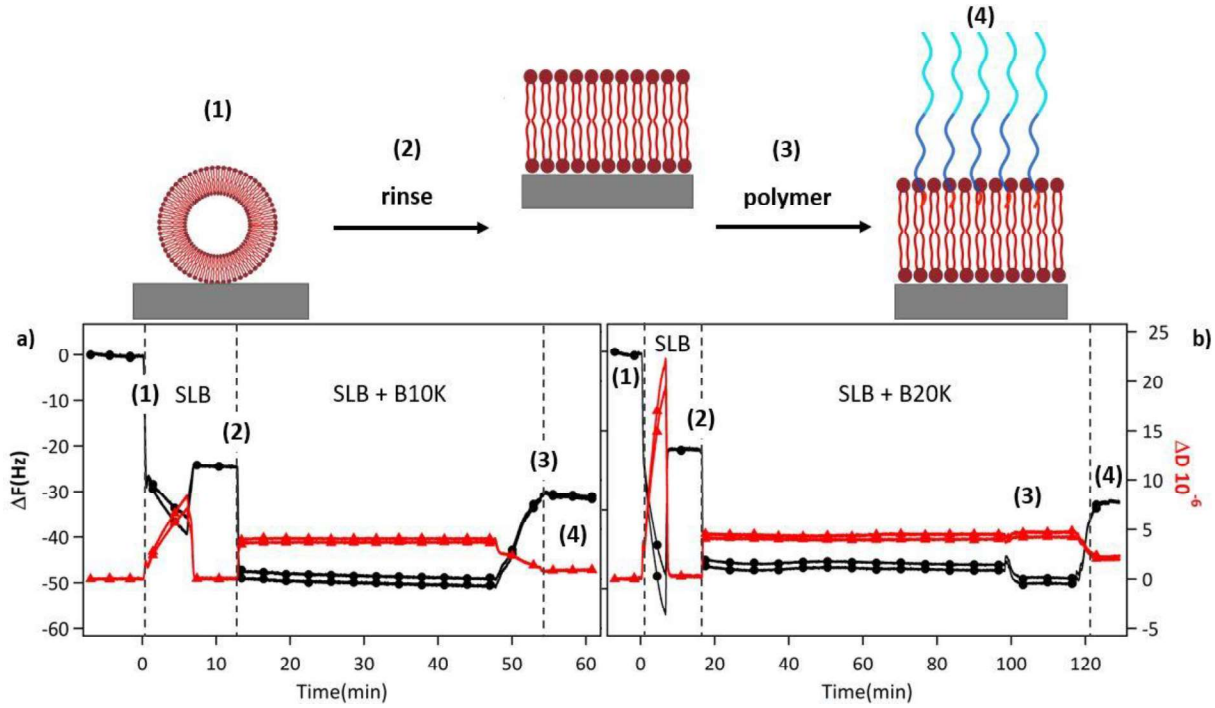

Figure 2. *PDMA-b-PNIPAM copolymers interaction with lipid bilayer through QCM-D measurements of the adsorption of the polymers B10K (a) and B20K (b) onto a DOPC supported lipid bilayer. Frequency variation measured for the 5th and 7th harmonics (black lines and filled circles), dissipation factors measured for the 5th and 7th harmonics (red lines and filled triangles). (1) DOPC vesicle injection flow 0.1 $mLmin^{-1}$ (t = 0), (2) rinse with water flow 0.1 $mLmin^{-1}$, (3) polymer addition flow 0.1 $mLmin^{-1}$, (4) rinse with water flow 0.1 $mLmin^{-1}$. This is a possible schematic representation of the polymer-lipid bilayer interaction.*

The interaction of B20K, which showed more efficient absorption onto the membrane, with DOPC lipid membranes was then studied in liposome dispersions, using DLS to monitor the effects of polymer inclusion and temperature on the hydrodynamic radius of liposomes. DLS measurements were performed on DOPC vesicles after 48h of interaction with the copolymer B20K, in the temperature range 25°-60°C (see SI for more details). Figure 3a displays the normalized

autocorrelation functions of the scattered intensity measured for DOPC-B20K at different temperatures.

The addition of the copolymer leads to a significant increase in the decay time of the autocorrelation functions (ACF) of the scattered intensity of liposomes, which corresponds to an increase in their hydrodynamic diameters from 90 to 120 nm (Figure S2, SI). Similarly to what was observed for SLBs, the copolymer is incorporated in the vesicles, resulting in an increase of their hydrodynamic thickness; as the temperature is increased, the decay time decreases more than expected (Figure 3a) from the regular dependence of diffusion coefficients on temperature, indicating a size decrease of the scattered objects. Figure 3b displays the hydrodynamic diameters of DOPC vesicle-B20K hybrids derived from the analysis of the ACFs, as well as the trend of average scattered intensity at a scattering angle of 90° as a function of temperature. The decrease of the hydrodynamic diameters occurs between 35°C and 50°C and levels off between 50°C and 55°C, with an inflection point at approximately 42°C, which corresponds to the volume phase transition of the PNIPAM block. As briefly sketched in Figure 3c, we can interpret this behaviour with the formation of a copolymer corona surrounding the vesicles. When T increases, the volume transition of the PNIPAM block determines the collapse of this corona, resulting in an overall size decrease of the scattered objects.

Interestingly, and particularly attractive for applicative purposes, this effect occurs in a relevant biological range, close to physiological conditions.

When the temperature is brought back to room conditions, the hydrodynamic radii reverts to its original value, indicating a reversibility of the process.

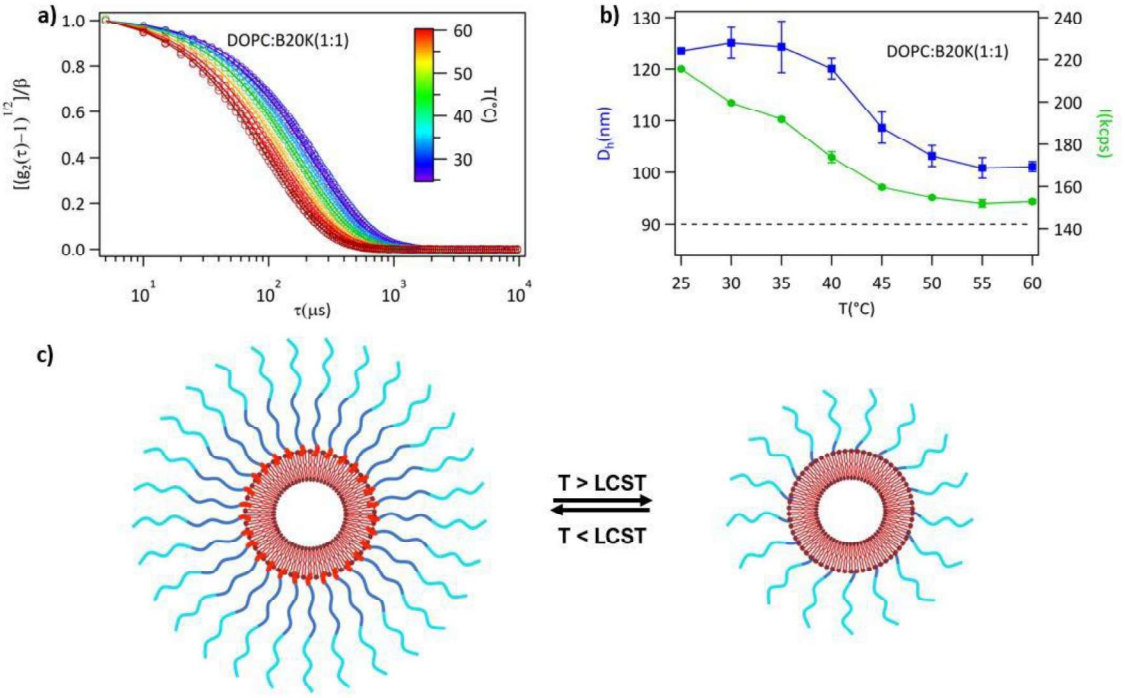

Figure 3. (a) Normalized intensity correlation functions of the DOPC vesicles stabilized with the polymer PDMA-b- PNIPAM B20K (1:1 w/w%) from 25°C to 60°C and the relative hydrodynamic radius and the count rate (b) as a function of temperature; segmented black line represents DOPC's hydrodynamic radius. Schematic representation of thermo-responsive DOPC/B20K nanoparticles (c); LCST represents the lower critical solution temperature of the NIPAM block.

From these experimental observations on the interactions between PDMA-*b*-PNIPAM and DOPC vesicles, it appears that the copolymer has a high affinity towards lipid membranes, where it spontaneously anchored and, maintains a significant thermo-responsiveness in a temperature range relevant for medical applications, unveiling reversible phenomenon.

3.2 PDMA-*b*-PNIPAM-stabilized cubosomes

Cubosome formulations of GMO with the two new stabilizers were prepared by adapting the method used with Pluronic F127 [46]. The formation of cubosomes was evaluated with DLS, using cubosomes stabilized with Pluronic F127 (lipid copolymer ratio 80/20 % w/w) as a reference. Figure 4 displays the ACF of GMO dispersions containing 20%, 33% and 50% (w/w) PDMA-*b*-PNIPAM

with respect to the lipid. From the ACFs it appears that colloidal dispersions of GMO were formed in all the investigated lipid/stabilizer compositions. The highest copolymer content (50%) creates the most stable and smallest monodispersed GMO nanoparticles, while as the copolymer content decreases, the hydrodynamic size of the particles increases and additional populations appear (histograms of the populations are reported in SI, Figure S4). While both B20K and B10K drive the formation of nanometric objects, nanoparticles stabilized by B20K were larger than those stabilized by B10K.

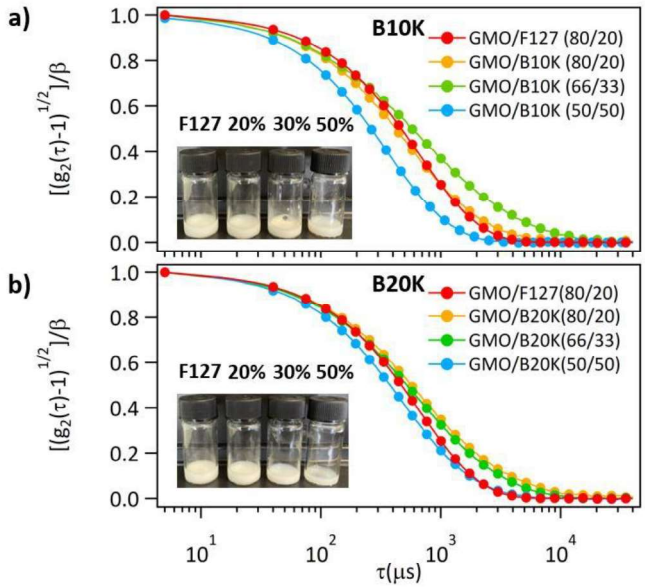

Figure 4. *Normalized intensity correlation function of the GMO dispersions with the polymer PDMA-b-PNIPAM B10K, Pluronic F127 (a) and the polymer B20K, Pluronic F127 (b), recorded at T = 25°C.*

The temperature-dependence of hydrodynamic size of cubosomes (see SI Figure S4) reveals a slight decrease in size in the range 25-50°C. The relative effect is smaller than that observed for DOPC vesicles, probably due to a higher complexity/polydispersity of the cubic nanoparticle dispersions with respect to liposomes. The size decrease of cubosomes when increasing temperature can be rationalized to the shrinkage of the copolymer corona around cubic nanoparticles, similarly to what discussed concerning DOPC liposomes, suggesting that the thermoresponsivity of the copolymer corona is retained also when stabilizing cubosomes.

To monitor the internal structure of cubosomes, we performed SAXS. First, the mesophase of the dispersions of the nanoparticles was surveyed for all the investigated lipid/polymer compositions at room temperature. As displayed in Figure 5, the stabilizer preserves the cubic phase of lipid/water systems only at the lower amounts of lipid/polymer ratio (80/20 in both cases and 66/33 for B20K),

since the loss of the characteristic Bragg peaks of a cubic phase occurs when the polymer content increases.

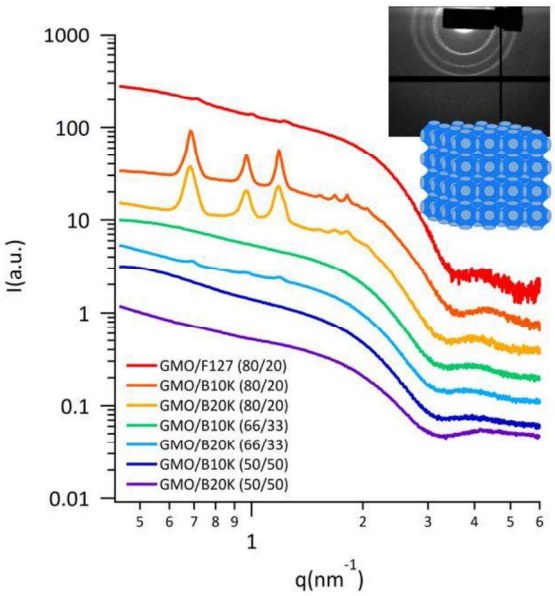

Figure 5. *SAXS curves of GMO dispersions stabilized with the polymer PDMA-b-PNIPAM B10K, B20K and Pluronic F127 at room temperature.*

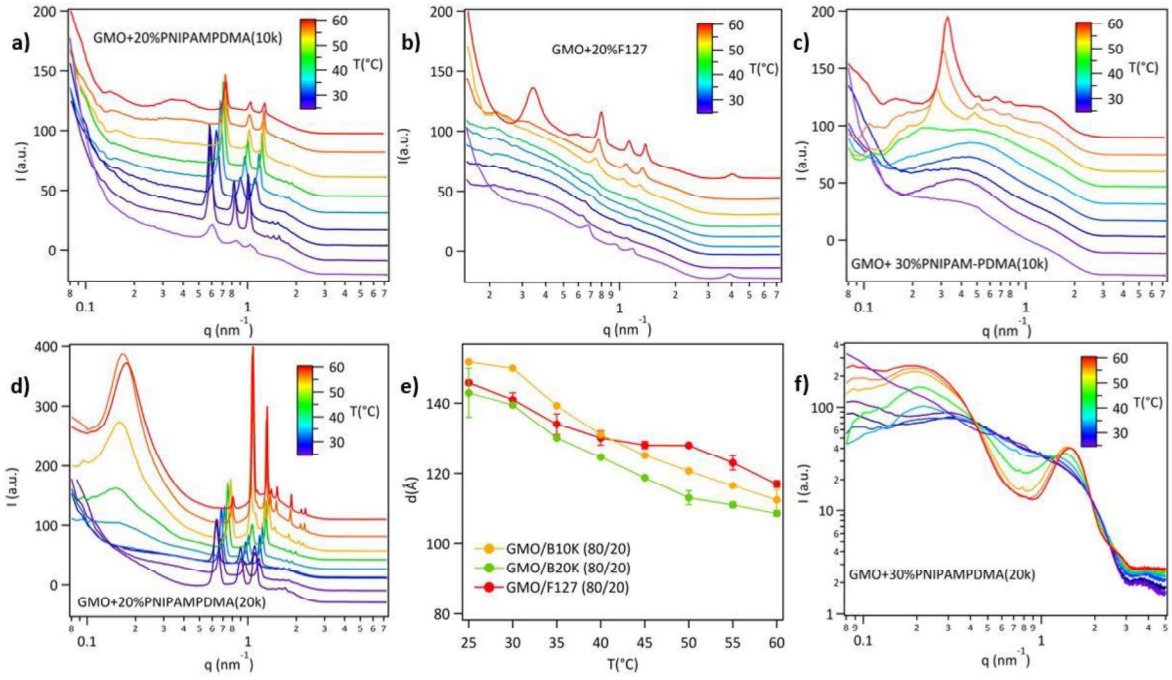

Figure 6*. SAXS curves of GMO dispersions stabilized with PDMA-b-PNIPAM B10K 20% (a)- 30% (c), B20K 20% (d)- 30 % (f) and Pluronic F127 20% (b) in the temperature range 25°C-60°C. Plots of the lattice parameteres (e) of the GMO cubosomes stabilized with the 20% of the polymer Pluronic F127, DMA-NIPAM (B10K) and PDMA-b-NIPAM (B20K) in the temperature range 25°C-60°C.*

Specifically, an ordered cubic phase, with a crystallographic space group of an *Im3m* and lattice parameters of d = 152 Å and d = 143 Å for B10K and B20K respectively, is observed when the lipid

is dispersed with a copolymer content of 20% for both polymers as displayed in Figure 5 [47]. These values are consistent with lattice parameters of 140 Å previously reported for primitive cubic phases stabilized with a similar amount of Pluronic [31]. It is known that copolymers used for dispersion and stabilization of cubosomes penetrate into the lipid bilayer influencing the internal organization of the lipids, and favoring a phase transition towards a less negatively curved phase (*Im3m*) with an increase of the lattice parameter [48–50]. In line with this observation, since the lattice parameter of the system GMO/PDMA-b-PNIPAM (80/20 % w/w) is higher at room temperature than the formulation GMO/Pluronic, we can hypothesize a stronger affinity of the copolymer in the first case. This is also supported by the loss of the inner liquid crystalline structure of GMO when the amount of copolymer is significantly increased. Interestingly, larger amounts of Pluronic F-127 (40 % (w/w)) are known to provoke a swelling of the phase yielding a phase transition from cubic to lamellar [51,52].

Thereafter, the temperature effect was evaluated on the inner organization of the lipid phase for the cubic formulations of GMO/polymer (80/20 and 66/33) (see Figure 6).

In all the GMO dispersions, a temperature increase causes the Bragg peaks of the *Im3m* cubic phase to shift to higher q-values, indicating a decrease of the lattice parameters and of the water channel radius (Figure 6 and Figure S6 in ESI). This temperature effect can be correlated with dehydration of the lipids due to reduced water-lipid polar head affinity. Noticeably, these modifications in the internal structure of the nanoparticles do not strongly affect the colloidal stability of the cubic particles, as proved by DLS measurements. Furthermore, for the formulation GMO/B20K 80/20 (w/w%) the coexistence of two distinct cubic phases, *Im3m* and *Pn3m*, arises from 50 to 60 °C, with channel's radii significantly smaller compared to cubosomes stabilized with Pluronic F127 (see Figure 6e). In summary, increasing the temperature leads to larger structural variations for the 80/20 (%w/w) GMO/B20K composition than for the corresponding GMO/B10K formulation (Figure S6 in ESI).

This result suggests that the GMO/PDMA-*b*-PNIPAM 80/20 (%w/w) is a promising DDS, due to the remarkable reduction of the water channel size as temperature increases, which means that 25% of the water volume within the original lipid nanoparticle is expelled as the copolymer go through its volume phase transition temperature. As a consequence, a proportional release of a hydrophilic cargo, originally confined in the water channels in the intact lipid nanoparticle, would be achieved thanks to this thermal response, via a sort of “sponge wringing effect” [53].

Cryo-TEM images of the dispersions GMO-B20K (80/20%) reveal a well-organized cubic structure possessing an organized architecture comparable to an *Im3m* structure [54] (Figure 7), as observed in the SAXS profiles. Square-shaped nanoparticles with cubic internal structure are formed in the size range from 100 to 300 nm, which is in good agreement with the hydrodynamic radius measured by

DLS. The nanoparticles are surrounded by flower-like vesicles, confirming a strong affinity of the polymer for lipid bilayers, which may also drive the formation of multiple vesicular structures co-existing with the cubic nanoparticles (see Figure 7a, b).

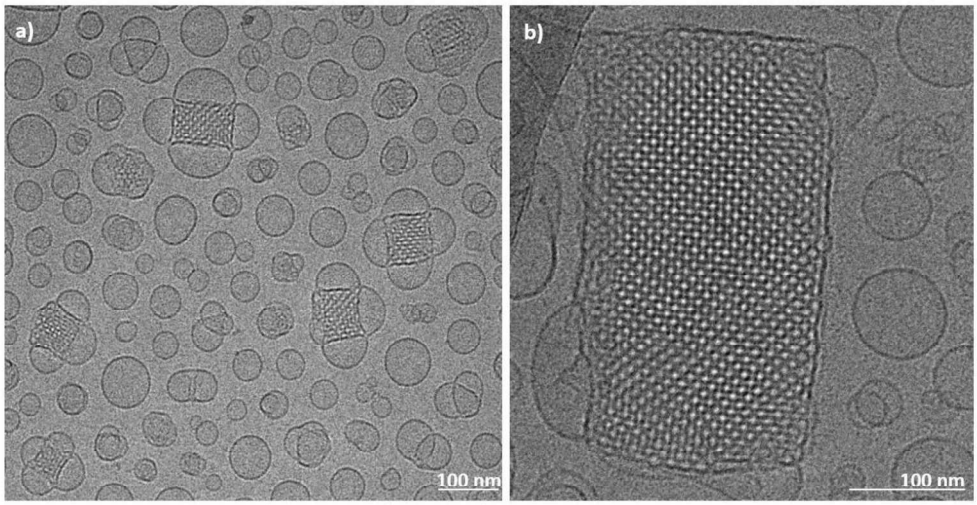

Figure 7. *Cryo-TEM images of cubosomes stabilized with the polymer PDMA-b-PNIPAM B20K (80/20) (a) and a single image of a cubosome (b).*

3.3 Interaction between PDMA-*b*-NIPAM-stabilized cubosomes and lipid membranes

The interaction between cubic nanoparticles and cellular membranes is crucial for their cellular uptake and therefore for therapeutic applications. So far, studies of cubosome affinity towards biorelevant interfaces have involved model membranes, such as supported lipid bilayers (SLBs) consisting of different phospholipids, to predict and unveil mechanisms involved in the interaction with cells with the aim of improving the design of biocompatible cubic formulations [55,56].

We tested the interaction of the cubosomal dispersion, consisting of cubosomes stabilized with PDMA-*b*-PNIPAM (20K) (80/20 w/w %), with a DOPC lipid membrane. DOPC, and phosphocholine lipids in general, are ubiquitous components of biological plasma membranes [57], and are therefore frequently used as highly simplified membrane models [58]. To evaluate the ability of PDMA-*b*-PNIPAM (20K)-stabilized cubosomes to interact with a DOPC membrane, we performed a QCM-D experiment in which we challenged DOPC SLBs with a dispersion of B20K-cubosomes (Figure 8a) or, as a reference, with a dispersion of Pluronic F-127 cubosomes (Figure 8b). The QCM-D graphs show that, for both experiments, incubation with the SLBs results in a significant increase (in absolute value) of both frequency shifts and dissipation factors. Upon rinsing, the adsorbed layer of PDMA-*b*-NIPAM (20K)-stabilized cubosomes was characterized by a frequency shift of -40 Hz and

dissipation of 6, while that of Pluronic F-127 cubosomes revealed a frequency shift of -30 Hz and dissipation of 2, consistent with a significantly lower adsorbed mass. The higher dissipation factors, indicate the formation of a more viscous layer when cubosomes adhere and fuse onto the lipid bilayer. The larger frequency and dissipation shifts observed for the PDMA-*b*-PNIPAM cubosomes prove a comparatively higher affinity of this hybrid system for biomimetic lipid membranes, suggesting a promising ability of the system to interact and, possibly, cross biological lipid interfaces to reach specific biological targets. The higher interaction displayed by the novel formulations can be correlated to the different chemical nature of the polymeric corona surrounding the cubosomes.

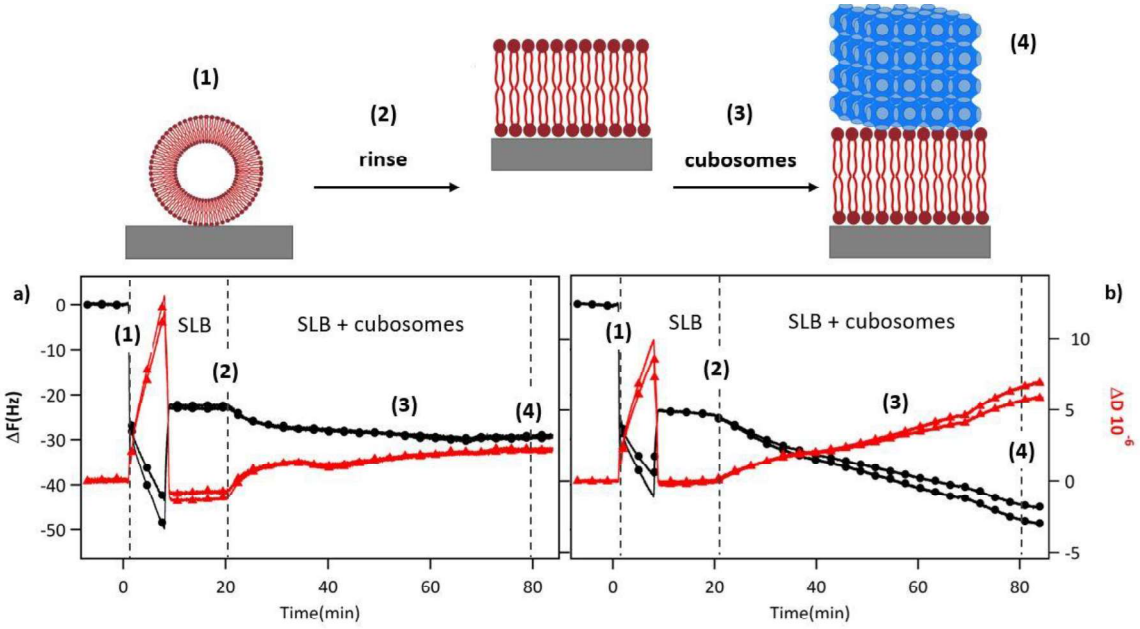

Figure 8. *QCM-D measurements of the absorption of the cubosomes stabilized with the polymer PDMA-b-PNIPAM(20K) (80/20) (a) and the polymer Pluronic F127 (b) onto DOPC SLB . Frequency variation measured for the 5th and 7th harmonics (black lines and filled circles), dissipation factors measured for the 5th and 7th harmonics (red lines and filled triangles). (1) DOPC vesicle injection flow 0.1 mLmin^{-1} (t = 0), (2) rinse with water flow 0.1 mLmin^{-1}, (3) cubosomes addition flow 0.1 mLmin^{-1}, (4) rinse with water flow 0.1 mLmin^{-1}.*

4. Conclusions

In this work we show that a recently synthesized thermoresponsive block copolymer, PDMA-*b*-PNIPAM, can be used to decorate lipid-based nanoparticles (either liposomes or cubosomes) to efficiently stabilize their dispersions in aqueous media. Its inclusion in the lipid bilayer monitored through QCM-D is spontaneous and prompted by the high affinity of the copolymer for the bilayer, also driven by the presence of an alkyl tag conjugated to the hydrophobic block. Not only the copolymer retains its responsiveness, but it also imparts thermal responsivity to the lipid nanoparticles (both liposomes and cubosomes), due to the collapse of the PNIPAM segment consequent of its volume phase transition.

As shown by scattering experiments (DLS and SAXS), changes in temperature in a physiologically relevant range induce both structural modification of the cubosome corona and of the cubic phase internal structure. The reversible shrinkage of the water channels, with release of the inner water phase, suggests a trigger mechanism for the release of hydrophilic cargoes for drug delivery applications.

Interestingly, PDMA-*b*-PNIPAM-stabilized cubosomes show a high affinity for biomimetic lipid membranes and a comparatively higher affinity with respect to GMO cubic nanoparticles stabilized by F127 as shown by QCM-D monitoring.

These last results suggest that these novel cubosomes may be able to first interact and fuse with plasma membranes, and then to release their cargo in the proximity to specific biological targets. Thanks to the combination of the temperature responsiveness of the system with the strong affinity towards lipid membranes, this new class of cubosomes stabilized with a thermo-responsive corona represents a promising candidate for applications as a smart, stimuli-responsive DDS.

CRediT authorship contribution statement

Arianna Balestri: Conceptualization, Methodology, Investigation, Writing – original draft & review. Barbara Lonetti: Conceptualization, Methodology, Investigation, Writing- review & editing. Simon Harrisson: Methodology, Writing- review. Barbara Farias-Mancilla: Investigation. Junliang Zhang: Investigation. Ulrich Schubert: Investigation. Heinz Amenitsh: Methodology, Investigation. Carlos Guerrero-Sanchez: Investigation. Costanza Montis: Conceptualization, Methodology, Writing- review & editing. Debora Berti: Conceptualization, Methodology, Writing - review & editing, Supervision, Funding acquisition.

Declaration of Competing Interest

The authors declare that they have no known competing financial interests or personal relationships that could have appeared to influence the work reported in this paper.

Acknowledgements

Funding: This work was supported by MIUR-Italy ("Progetto Dipartimenti di Eccellenza 2018–2022, allocated to Department of Chemistry "Ugo Schiff"). The authors acknowledge the CERIC-ERIC Consortium for the access to experimental facilities and the beam time. The authors thank the technical support in Cryo-TEM measurements performed in the FloCEN Florence Center for Electron Nanoscopy of the University of Florence. All the authors acknowledge Pietro Grazi for his contribution on DLS measurements of cubosomes stabilized by F127. S.H, B.F.M. and BL acknowledge the Agence Nationale de la Recherche (ANR, France, ANR project: ANR-15-CE08-

0039). C.G.- S. and U.S.S. gratefully acknowledge the support of the Deutsche Forschungsgemeinschaft (DFG, Germany) for funding through the Collaborative Research Centre Poly-Target (Project No. 316213987, SFB 1278, Projects B02, Z01 and A04).

References

[1] G. Tiwari, R. Tiwari, S. Bannerjee, L. Bhati, S. Pandey, P. Pandey, B. Sriwastawa, Drug delivery systems: An updated review, Int. J. Pharm. Investig. 2 (2012) 2. https://doi.org/10.4103/2230-973x.96920.

[2] O.M. Koo, I. Rubinstein, H. Onyuksel, Role of nanotechnology in targeted drug delivery and imaging: a concise review, Nanomedicine Nanotechnology, Biol. Med. 1 (2005) 193–212. https://doi.org/10.1016/j.nano.2005.06.004.

[3] A.Z. Wilczewska, K. Niemirowicz, K.H. Markiewicz, H. Car, Nanoparticles as drug delivery systems, Pharmacol. Reports. 64 (2012) 1020–1037. https://doi.org/10.1016/S1734-1140(12)70901-5.

[4] G. Pillai, Nanomedicines for Cancer Therapy: An Update of FDA Approved and Those under Various Stages of Development, SOJ Pharm. Pharm. Sci. (2014). https://doi.org/10.15226/2374-6866/1/2/00109.

[5] D. Bobo, K.J. Robinson, J. Islam, K.J. Thurecht, S.R. Corrie, Nanoparticle-Based Medicines: A Review of FDA-Approved Materials and Clinical Trials to Date, Pharm. Res. 33 (2016) 2373–2387. https://doi.org/10.1007/s11095-016-1958-5.

[6] A. Wang-Gillam, C.P. Li, G. Bodoky, A. Dean, Y.S. Shan, G. Jameson, T. MacArulla, K.H. Lee, D. Cunningham, J.F. Blanc, R.A. Hubner, C.F. Chiu, G. Schwartsmann, J.T. Siveke, F. Braiteh, V. Moyo, B. Belanger, N. Dhindsa, E. Bayever, D.D. Von Hoff, L.T. Chen, Nanoliposomal irinotecan with fluorouracil and folinic acid in metastatic pancreatic cancer after previous gemcitabine-based therapy (NAPOLI-1): A global, randomised, open-label, phase 3 trial, Lancet. 387 (2016) 545–557. https://doi.org/10.1016/S0140-6736(15)00986-1.

[7] I.M. Hann, H.G. Prentice, Lipid-based amphotericin B: A review of the last 10 years of use, Int. J. Antimicrob. Agents. 17 (2001) 161–169. https://doi.org/10.1016/S0924-8579(00)00341-1.

[8] Y. Li, R. Tenchov, J. Smoot, C. Liu, S. Watkins, Q. Zhou, A Comprehensive Review of the Global Efforts on COVID-19 Vaccine Development, ACS Cent. Sci. 2 (2021). https://doi.org/10.1021/acscentsci.1c00120.

[9] B. Ozpolat, A.K. Sood, G. Lopez-Berestein, Liposomal siRNA nanocarriers for cancer therapy, Adv. Drug Deliv. Rev. 66 (2014) 110–116. https://doi.org/10.1016/j.addr.2013.12.008.

[10] R. Negrini, R. Mezzenga, Diffusion , Molecular Separation , and Drug Delivery from Lipid Mesophases with Tunable Water Channels, Langmuir. 28 (n.d.) 16455−16462.

[11] X. Mulet, B.J. Boyd, C.J. Drummond, Advances in drug delivery and medical imaging using colloidal lyotropic liquid crystalline dispersions, J. Colloid Interface Sci. 393 (2013) 1–20. https://doi.org/10.1016/j.jcis.2012.10.014.

[12] R. Negrini, W.K. Fong, B.J. Boyd, R. Mezzenga, PH-responsive lyotropic liquid crystals and their potential therapeutic role in cancer treatment, Chem. Commun. 51 (2015) 6671–6674.

https://doi.org/10.1039/c4cc10274f.

[13] W. Fong, R. Negrini, J.J. Vallooran, R. Mezzenga, B.J. Boyd, Responsive self-assembled nanostructured lipid systems for drug delivery and diagnostics, J. Colloid Interface Sci. 484 (2016) 320–339. https://doi.org/10.1016/j.jcis.2016.08.077.

[14] M. Mendozza, A. Balestri, C. Montis, D. Berti, Controlling the kinetics of an enzymatic reaction through enzyme or substrate confinement into lipid mesophases with tunable structural parameters, Int. J. Mol. Sci. 21 (2020) 1–16. https://doi.org/10.3390/ijms21145116.

[15] C. Montis, B. Castroflorio, M. Mendozza, A. Salvatore, D. Berti, P. Baglioni, Magnetocubosomes for the delivery and controlled release of therapeutics, J. Colloid Interface Sci. 449 (2015). https://doi.org/10.1016/j.jcis.2014.11.056.

[16] A. Zabara, R. Mezzenga, Controlling molecular transport and sustained drug release in lipid-based liquid crystalline mesophases, J. Control. Release. 188 (2014) 31–43. https://doi.org/10.1016/j.jconrel.2014.05.052.

[17] K.W.Y. Lee, T.H. Nguyen, T. Hanley, B.J. Boyd, Nanostructure of liquid crystalline matrix determines in vitro sustained release and in vivo oral absorption kinetics for hydrophilic model drugs, Int. J. Pharm. 365 (2009) 190–199. https://doi.org/10.1016/j.ijpharm.2008.08.022.

[18] M.J. Lawrence, Surfactant systems: Their use in drug delivery, Chem. Soc. Rev. 23 (1994) 417–424. https://doi.org/10.1039/CS9942300417.

[19] I.D.M. Azmi, S.M. Moghimi, A. Yaghmur, Cubosomes and hexosomes as versatile platforms for drug delivery, Ther. Deliv. 6 (2015) 1347–1364. https://doi.org/10.4155/tde.15.81.

[20] H.M.G. Barriga, M.N. Holme, M.M. Stevens, Cubosomes: The Next Generation of Smart Lipid Nanoparticles?, Angew. Chemie - Int. Ed. 58 (2019) 2958–2978. https://doi.org/10.1002/anie.201804067.

[21] L. Boge, H. Bysell, L. Ringstad, D. Wennman, A. Umerska, V. Cassisa, J. Eriksson, M.L. Joly-Guillou, K. Edwards, M. Andersson, Lipid-Based Liquid Crystals As Carriers for Antimicrobial Peptides: Phase Behavior and Antimicrobial Effect, Langmuir. 32 (2016) 4217–4228. https://doi.org/10.1021/acs.langmuir.6b00338.

[22] C. Caltagirone, A.M. Falchi, S. Lampis, V. Lippolis, V. Meli, M. Monduzzi, L. Prodi, J. Schmidt, M. Sgarzi, Y. Talmon, R. Bizzarri, S. Murgia, Cancer-cell-targeted theranostic cubosomes, Langmuir. 30 (2014) 6228–6236. https://doi.org/10.1021/la501332u.

[23] G. Zhen, T.M. Hinton, B.W. Muir, S. Shi, M. Tizard, K.M. McLean, P.G. Hartley, P. Gunatillake, Glycerol monooleate-based nanocarriers for siRNA delivery in vitro, Mol. Pharm. 9 (2012) 2450–2457. https://doi.org/10.1021/mp200662f.

[24] S. Murgia, S. Biffi, R. Mezzenga, Recent advances of non-lamellar lyotropic liquid crystalline nanoparticles in nanomedicine, Curr. Opin. Colloid Interface Sci. 48 (2020) 28–39. https://doi.org/10.1016/j.cocis.2020.03.006.

[25] M. Valldeperas, A. Salis, J. Barauskas, F. Tiberg, T. Arnebrant, V. Razumas, M. Monduzzi, T. Nylander, Enzyme encapsulation in nanostructured self- assembled structures : Toward biofunctional supramolecular assemblies, Curr. Opin. Colloid Interface Sci. 44 (2019) 130–142. https://doi.org/10.1016/j.cocis.2019.09.007.

[26] C. Fong, T. Le, C.J. Drummond, C. Fong, Lyotropic liquid crystal engineering–ordered nanostructured small molecule amphiphile self-assembly materials by design, Chem. Soc.

Rev. 41 (2012) 1297–1322. https://doi.org/10.1039/c1cs15148g.

[27] S.P. Akhlaghi, I.R. Ribeiro, B.J. Boyd, W. Loh, Impact of preparation method and variables on the internal structure, morphology, and presence of liposomes in phytantriol-Pluronic® F127 cubosomes, Colloids Surfaces B Biointerfaces. 145 (2016) 845–853. https://doi.org/10.1016/j.colsurfb.2016.05.091.

[28] J.Y.T. Chong, X. Mulet, B.J. Boyd, Steric Stabilizers for Cubic Phase Lyotropic Liquid Crystal Nanodispersions (Cubosomes), 1st ed., Elsevier Inc., 2015. https://doi.org/10.1016/bs.adplan.2014.11.001.

[29] K. Lindell, J. Engblom, M. Jonströmer, A. Carlsson, S. Engström, Influence of a charged phospholipid on the release pattern of timolol maleate from cubic liquid crystalline phases, Prog. Colloid Polym. Sci. 108 (1998) 111–118. https://doi.org/10.1007/bfb0117968.

[30] A. Tan, L. Hong, J.D. Du, B.J. Boyd, Self-Assembled Nanostructured Lipid Systems: Is There a Link between Structure and Cytotoxicity?, Adv. Sci. 6 (2019). https://doi.org/10.1002/advs.201801223.

[31] J.Y.T. Chong, X. Mulet, L.J. Waddington, B.J. Boyd, C.J. Drummond, Steric stabilisation of self-assembled cubic lyotropic liquid crystalline nanoparticles: High throughput evaluation of triblock polyethylene oxide-polypropylene oxide-polyethylene oxide copolymers, Soft Matter. 7 (2011) 4768–4777. https://doi.org/10.1039/c1sm05181d.

[32] J. Zhai, T.M. Hinton, L.J. Waddington, C. Fong, N. Tran, X. Mulet, C.J. Drummond, B.W. Muir, Lipid-PEG Conjugates Sterically Stabilize and Reduce the Toxicity of Phytantriol-Based Lyotropic Liquid Crystalline Nanoparticles, Langmuir. 31 (2015) 10871–10880. https://doi.org/10.1021/acs.langmuir.5b02797.

[33] M. Fornasier, S. Biffi, B. Bortot, P. Macor, A. Manhart, F.R. Wurm, S. Murgia, Cubosomes stabilized by a polyphosphoester-analog of Pluronic F127 with reduced cytotoxicity, J. Colloid Interface Sci. 580 (2020) 286–297. https://doi.org/10.1016/j.jcis.2020.07.038.

[34] M. Chountoulesi, N. Pippa, V. Chrysostomou, S. Pispas, D.E. Chrysina, A. Forys, L. Otulakowski, B. Trzebicka, C. Demetzos, Stimuli-Responsive Lyotropic Liquid Crystalline Nanosystems with Incorporated Poly(2-Dimethylamino Ethyl Methacrylate)-b-Poly(Lauryl Methacrylate) Amphiphilic Block Copolymer, Polymers (Basel). 11 (2019) 1400.

[35] M. Kluzek, A.I.. Tyler, S. Wang, R. Chen, C.M. Marques, F. Thalmann, J.M. Seddon, M. Schmutz, Influence of a pH-sensitive polymer on the structure of monoolein cubosomes, Soft Matter. 13 (2017) 7571–7577. https://doi.org/10.1039/C7SM01620D.

[36] M. Chountoulesi, D.R. Perinelli, A. Forys, G. Bonacucina, B. Trzebicka, S. Pispas, C. Demetzos, Liquid crystalline nanoparticles for drug delivery: The role of gradient and block copolymers on the morphology, internal organisation and release profile, Eur. J. Pharm. Biopharm. 158 (2021) 21–34. https://doi.org/10.1016/j.ejpb.2020.08.008.

[37] A. Halperin, M. Kröger, F.M. Winnik, Poly(N-isopropylacrylamide) Phase Diagrams: Fifty Years of Research, Angew. Chemie - Int. Ed. 54 (2015) 15342–15367. https://doi.org/10.1002/anie.201506663.

[38] A. Polozova, F.M. Winnik, Contribution of hydrogen bonding to the association of liposomes and an anionic hydrophobically modified poly(N-isopropylacrylamide), Langmuir. 15 (1999) 4222–4229. https://doi.org/10.1021/la9804839.

[39] I. Kolman, N. Pippa, A. Meristoudi, S. Pispas, C. Demetzos, A dual-stimuli-responsive polymer into phospholipid membranes: A thermotropic approach, J. Therm. Anal. Calorim.

123 (2016) 2257–2271. https://doi.org/10.1007/s10973-015-5080-4.

[40] C. Montis, B. Castroflorio, M. Mendozza, A. Salvatore, D. Berti, P. Baglioni, Magnetocubosomes for the delivery and controlled release of therapeutics, J. Colloid Interface Sci. 449 (2015) 317–326. https://doi.org/10.1016/j.jcis.2014.11.056.

[41] S.W. Provencher, Contin: a general purpose constrained regularization program for inverting noisy linear algebraic and integral equations, Comput. Phys. Communcations. 27 (1982) 229–242.

[42] A. Balestri, L. Chiappisi, C. Montis, S. Micciulla, B. Lonetti, D. Berti, Organized Hybrid Molecular Films from Natural Phospholipids and Synthetic Block Copolymers: A Physicochemical Investigation, Langmuir. 36 (2020) 10941–10951. https://doi.org/10.1021/acs.langmuir.0c01544.

[43] L.R. Jordan, M.E. Blauch, A.M. Baxter, J.L. Cawley, N.J. Wittenberg, Influence of brain gangliosides on the formation and properties of supported lipid bilayers, Colloids Surfaces B Biointerfaces. 183 (2019) 110442. https://doi.org/10.1016/j.colsurfb.2019.110442.

[44] C. Montis, Y. Gerelli, G. Fragneto, T. Nylander, P. Baglioni, D. Berti, Nucleolipid bilayers : A quartz crystal microbalance and neutron reflectometry study, Colloids Surfaces B Biointerfaces. 137 (2016) 203–213.

[45] R. Richter, A. Mukhopadhyay, A. Brisson, Pathways of Lipid Vesicle Deposition on Solid Surfaces: A Combined QCM-D and AFM Study, Biophys. J. 85 (2003) 3035–3047. https://doi.org/10.1016/S0006-3495(03)74722-5.

[46] C. Guo, J. Wang, F. Cao, R.J. Lee, G. Zhai, Lyotropic liquid crystal systems in drug delivery, Drug Discov. Today. 15 (2010) 1032–1040. https://doi.org/10.1016/j.drudis.2010.09.006.

[47] F. Caboi, G.S. Amico, P. Pitzalis, M. Monduzzi, T. Nylander, K. Larsson, Addition of hydrophilic and lipophilic compounds of biological relevance to the monoolein/water system. I. Phase behavior, Chem. Phys. Lipids. 109 (2001) 47–62. https://doi.org/10.1016/S0009-3084(00)00200-0.

[48] J. Zhai, S. Sarkar, C.E. Conn, C.J. Drummond, Molecular engineering of super-swollen inverse bicontinpus cubic and sponge lipid phases for biomedical applications, Mol. Syst. Des. Eng. (2020). https://doi.org/10.1039/d0me00076k.

[49] L. Van'T Hag, S.L. Gras, C.E. Conn, C.J. Drummond, Lyotropic liquid crystal engineering moving beyond binary compositional space-ordered nanostructured amphiphile self-assembly materials by design, Chem. Soc. Rev. 46 (2017) 2705–2731. https://doi.org/10.1039/c6cs00663a.

[50] J. Zhai, S. Sarkar, C.E. Conn, C.J. Drummond, Molecular engineering of super-swollen inverse bicontinuous cubic and sponge lipid phases for biomedical applications, Mol. Syst. Des. Eng. (2020).

[51] J. Gustafsson, H. Ljusberg-Wahren, M. Almgren, K. Larsson, Submicron particles of reversed lipid phases in water stabilized by a nonionic amphiphilic polymer, Langmuir. 13 (1997) 6964–6971. https://doi.org/10.1021/la970566+.

[52] T. Landh, Phase behavior in the system pine oil monoglycerides-poloxamer 407-water at 20°C, J. Phys. Chem. 98 (1994) 8453–8467. https://doi.org/10.1021/j100085a028.

[53] M. Mendozza, C. Montis, L. Caselli, M. Wolf, P. Baglioni, D. Berti, On the thermotropic and magnetotropic phase behavior of lipid liquid crystals containing magnetic nanoparticles,

Nanoscale. 10 (2018) 3480–3488. https://doi.org/10.1039/c7nr08478a.

[54] D. Danino, Cryo-TEM of soft molecular assemblies, Curr. Opin. Colloid Interface Sci. 17 (2012) 316–329. https://doi.org/10.1016/j.cocis.2012.10.003.

[55] B.P. Dyett, H. Yu, J. Strachan, C.J. Drummond, C.E. Conn, Fusion dynamics of cubosome nanocarriers with model cell membranes, Nat. Commun. 10 (2019). https://doi.org/10.1038/s41467-019-12508-8.

[56] P. Vandoolaeghe, A.R. Rennie, R.A. Campbell, R.K. Thomas, F. Höök, G. Fragneto, F. Tiberg, T. Nylander, Adsorption of cubic liquid crystalline nanoparticles on model membranes, Soft Matter. 4 (2008) 2267–2277. https://doi.org/10.1039/b801630e.

[57] G. Van Meer, D.R. Voelker, G.W. Feigenson, Membrane lipids: Where they are and how they behave, Nat. Rev. Mol. Cell Biol. 9 (2008) 112–124. https://doi.org/10.1038/nrm2330.

[58] M. Kang, M. Tuteja, A. Centrone, D. Topgaard, C. Leal, Nanostructured Lipid-Based Films for Substrate-Mediated Applications in Biotechnology, Adv. Funct. Mater. 28 (2018) 1704356.

Declaration of interests

☒The authors declare that they have no known competing financial interests or personal relationships that could have appeared to influence the work reported in this paper.

☐The authors declare the following financial interests/personal relationships which may be considered as potential competing interests:

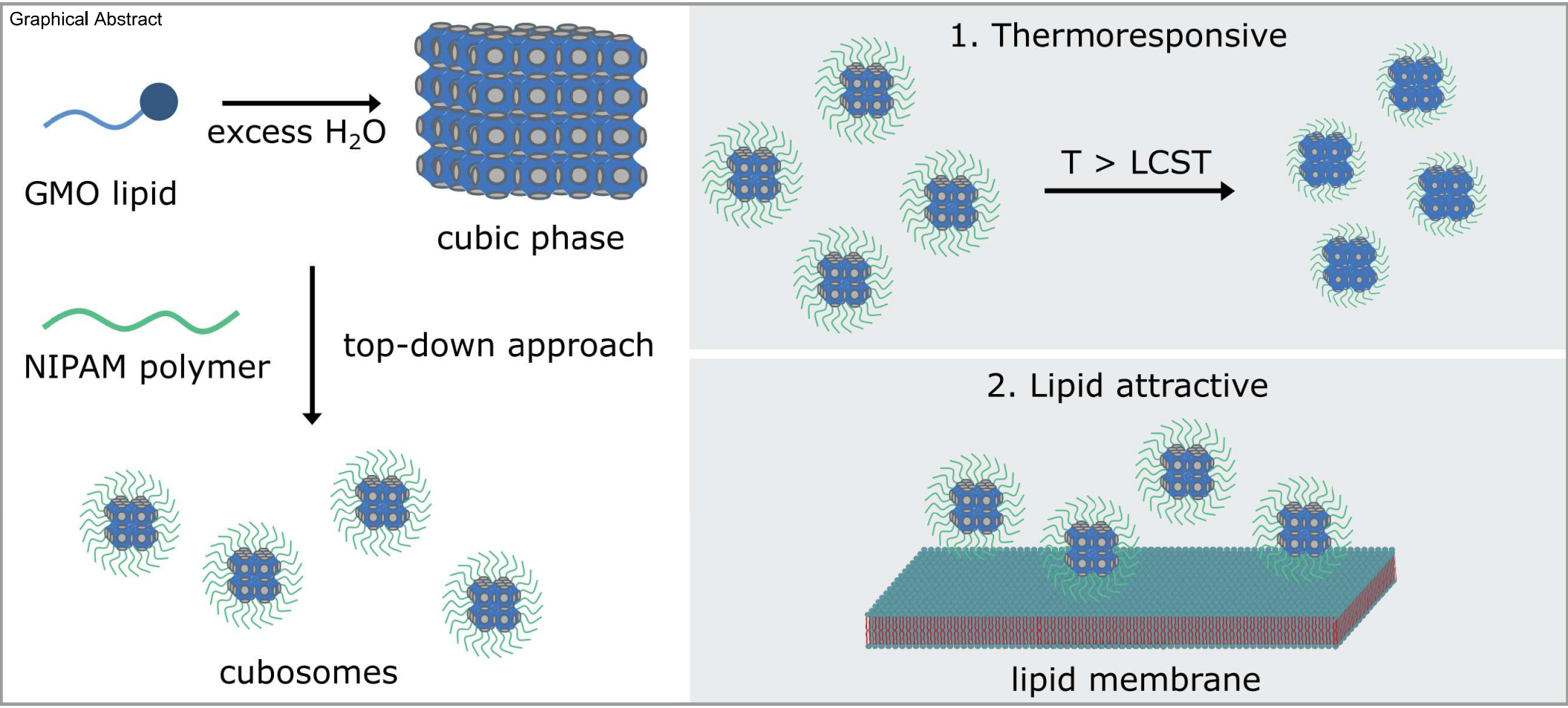
Graphical Abstract
excess H_2O
GMO lipid
cubic phase
NIPAM polymer
top-down approach
cubosomes
1. Thermoresponsive
T > LCST
2. Lipid attractive
lipid membrane